



ELSEVIER

Catalysis Today 43 (1998) 89–99

**C** TODAY  
CATALYSIS  
TODAY

## Solid base catalysts for mercaptan oxidation

Joseph J. Alcaraz, Blaise J. Arena, Ralph D. Gillespie, Jennifer S. Holmgren<sup>\*</sup>

*UOP Research Center, 50E. Algonquin Road, Des Plaines, IL, USA*

### Abstract

Aqueous alkali can be completely replaced in the mercaptan oxidation reaction by incorporating solid basic materials into the catalyst formulation. The ability to use a solid oxide base to replace aqueous alkali will have a positive environmental impact because aqueous alkalis, such as caustic, are becoming a serious disposal problem for petroleum refiners and chemical manufacturers. The basic oxide system used contains cobalt phthalocyanine (CoPc) supported on a metal oxide solid solution (MOSS). Although active for mercaptan oxidation, this catalyst does not meet the lifetime requirements for commercial application. Three deactivation mechanisms have been identified: rehydration of the MOSS back to the layered double hydroxide (LDH) (because this rehydration causes a reduction in the basicity of these materials), deactivation by adsorption of heavy hydrocarbon species in the feed, and irreversible adsorption of acidic species from the feed. Knowledge of the deactivation mechanisms has allowed the design of a process that meets the required catalyst lifetime requirements. This process represents one of the first applications of solid base catalysis to a commercial process. Catalyst performance, factors affecting deactivation, and methods of preventing deactivation are discussed. © 1998 Elsevier Science B.V. All rights reserved.

### 1. Introduction

Caustic has been a mainstay in the oil refinery since the earliest days of the refining industry because it is very effective in removing acidic components, such as mercaptans, H<sub>2</sub>S, phenols, and inorganic or naphthenic acids from crude oil or its fractions. This effectiveness and the low cost of fresh caustic are the reasons for its widespread use. Now, the situation is changing in most parts of the world.

A fundamental problem is associated with the use of caustic in the refinery: caustic is not converted to a valuable product. Even worse, it must be discarded at a cost. This situation represents an inefficient use of raw material resources, and this inefficiency decreases refinery profit margins. Overcoming this situation

requires minimizing or eliminating the use of caustic wherever possible or treating spent caustic on-site if necessary.

Sulfidic caustic is recognized as a hazardous material because of its following characteristics; it is corrosive (high pH), it can contain toxic compounds, for example, H<sub>2</sub>S or phenol, and it places high biological and chemical oxygen demand (BOD and COD) on natural water environments.

Due to the nature of spent caustic, environmental agencies around the world have tightened the regulations aimed at controlling its disposal. In consequence, the disposal of spent caustic has become difficult and often is expensive.

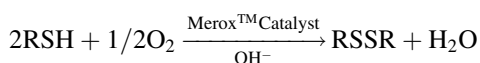
Several factors contribute to a refinery's total caustic cost: the purchase of fresh caustic, the loss of the hydrocarbon product during caustic scrubbing, the cost of handling all caustic within the refinery, and

<sup>\*</sup>Corresponding author.

the cost associated with paid outside disposal or treatment of spent caustic. In addition, some costs associated with caustic use are not easily measured in dollars. For example, safety issues involved in caustic handling can create significant, but intangible, costs.

All of these cost factors affect various refineries in differing degrees. For example, the costs of outside disposal can vary widely among refiners, depending on differing environmental regulations at both the national and local level. Further variations can result from the limitations on disposal options that may be available locally. The result of this situation is that the disposal of spent caustic can range from \$0.03 to \$0.53/l. As a typical refinery can generate 3,000,000 l/year of spent caustic, these costs can be significant.

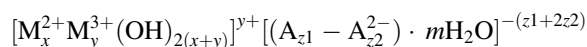
One of the major uses of caustic in the refinery is as a co-catalyst for the sweetening, the conversion of mercaptans (RSH) to disulfides (RSSR), of gasoline and kerosine ([1]);



The environmental and economic advantages of eliminating the use of caustic in mercaptan sweetening and thus attaining an effluent-free system led to the investigation of using solid rather than liquid bases as co-catalysts for this reaction.

One possible route to replace caustic is the use of basic solid oxides such as LDHs. Substantial data in the literature suggest that these materials are useful for reactions normally catalyzed by aqueous base, including aldol condensation, ethylene polymerization, alcohol synthesis, and hydrolysis of nitriles [2]. As with other solid oxides, the expectation is that these materials would be regenerable. The LDHs have a Brucite-like structure. This structure consists of stacked hydroxyl layers or sheets composed of edge-sharing octahedra and an interlamellar space separating the layers. If the layer does not contain a trivalent metal cation or any other cations of greater than +2 oxidation state, then the layer is neutral. This situation is exactly the case for Brucite ( $\text{Mg}(\text{OH})_2$ ). In LDHs, the charge is generated by the substitution of a divalent metal cation by a more highly charged (usually a trivalent) metal cation. Each substitution by a trivalent cation translates into a net gain of a positive charge for the layer (Fig. 1). This layer charge is counterbalanced by anions in the interlayer spaces.

LDHs include a wide variety of compositions. The general formula for this material is



where octahedral sites are  $\text{M}^{2+} \Rightarrow \text{Mg}, \text{Ni}, \text{Zn}, \text{Co}, \text{Fe}$ ,

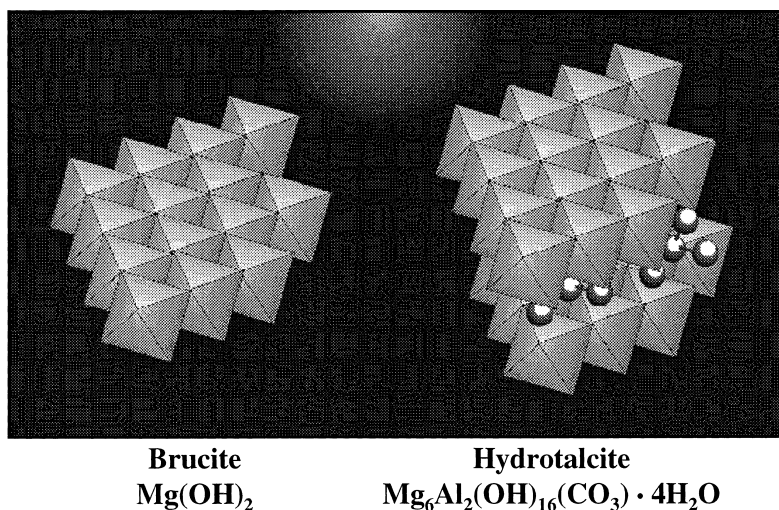


Fig. 1. Comparison of Brucite and Hydrotalcite. Hydrotalcite has the same structure and connectivity as Brucite. In Hydrotalcite, the substitution of a +3 Al cation results in a net positive layer charge. For this reason, interlayer anions are needed to compensate the charge.

$\text{Cu}$ ,  $\text{M}^{3+} \Rightarrow \text{Al}$ ,  $\text{Fe}$ ,  $\text{Cr}$  and counterbalancing anions are  $\text{A} \Rightarrow \text{CO}_3^{2-}$ ,  $\text{SO}_4^{2-}$ ,  $\text{NO}_3^-$ ,  $\text{Cl}^-$ ,  $\text{Br}^-$ ,  $\text{ClO}_4^-$ ,  $\text{I}^-$ ,  $\text{F}^-$ ,  $\text{OH}^-$ .

LDHs of a variety of compositions are found in nature. For example, the mineral with the composition of  $\text{Mg}_6\text{Al}_2(\text{OH})_{16}\text{CO}_3 \cdot 4\text{H}_2\text{O}$  is called Hydrotalcite; that with the composition  $\text{Ni}_6\text{Al}_2(\text{OH})_{16}(\text{CO}_3) \cdot 4\text{H}_2\text{O}$ , Takovite; and that with composition  $\text{Mg}_6\text{Fe}_2(\text{OH})_{16}(\text{CO}_3) \cdot 4\text{H}_2\text{O}$ , Pyroaurite. These materials can also be easily synthesized and are relatively inexpensive to prepare in the laboratory.

The physical and chemical properties of LDHs can be controlled by their preparation route. LDHs have been prepared in the laboratory with different  $\text{M}^{2+}/\text{M}^{3+}$  ratios (1.7–4) and various compositions [3,4]. Two distinct synthesis routes are described in the literature: co-precipitation [5–8] and hydrothermal synthesis [9]. In general, higher temperature and longer heating time result in larger clay crystals. Lower temperature precipitations result in microcrystals of approximately 100 Å, and higher temperature (200°C) preparations result in crystals in the range of 0.2–0.5 µm. Lower crystallinity corresponds to higher surface areas. Activation temperatures in the range of 400–600°C yield the optimum surface areas of about 200–300 m<sup>2</sup>/g.

The LDH itself, although an anion exchanger, is not as basic as the metal oxide formed on calcination of the LDH. UOP terms this material MOSS because its X-ray diffraction (XRD) pattern resembles a metal oxide solid solution (MOSS) of the constituent oxides (Fig. 2). Characterization and reactivity data suggest that the MOSS is a strong base and is the active ingredient in base-catalyzed reactions using LDH precursors. The synthesis and the chemical and physical properties of LDHs have been extensively reviewed [10].

## 2. Experimental

### 2.1. LDH preparation

All LDHs were prepared using the low-temperature precipitation methods first introduced by Feitknecht in the 1930s [6–8]. Essentially, the di- and tri-valent metal cation salts are added to a sodium hydroxide and carbonate solution. Homogeneous products are obtained if the components are added slowly and

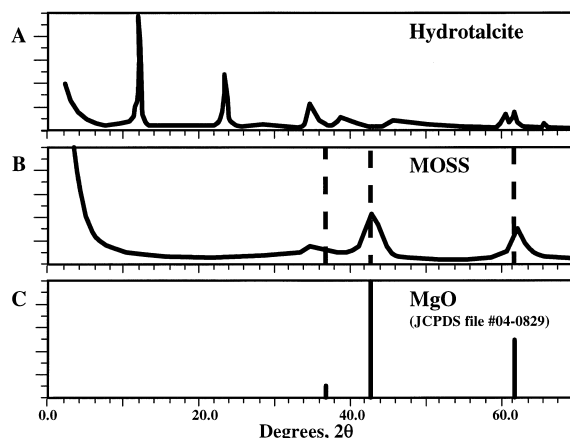


Fig. 2. The XRD patterns for Hydrotalcite and for a Mg–Al MOSS. Note that a comparison of the MOSS XRD pattern and that of the stick pattern for MgO shows that the MOSS is shifted relative to the MgO. This result is due to the formation of a metal oxide solid solution of the component oxides ( $\text{MgO}$  and  $\text{Al}_2\text{O}_3$ ).

mixed vigorously. The addition is carried out at 0°C to further control precipitation. Subsequently, the gel is heated to 60–70°C; this temperature is maintained for 12–16 h. The product is recovered and washed by filtration and then dried at 100°C.

Activation of the LDH is accomplished by heating to temperatures above 300°C for several hours in air. Standard conditions for this experiment include heating to 450°C for 6 h in flowing air. In these conditions, the LDHs are completely converted to the MOSS.

#### 2.1.1. Preparation of $\text{MgO}/\text{Al}_2\text{O}_3$ solid solution

A 2 l, three-necked round-bottomed flask was equipped with a reflux condenser, a thermometer, and a mechanical stirrer. To this flask was added a solution containing 610 g of water, 60 g of  $\text{Na}_2\text{CO}_3 \cdot \text{H}_2\text{O}$  and 71 g of  $\text{NaOH}$  and the flask was cooled to <5°C. An addition funnel containing 345 g water, 130 g of  $\text{Mg}(\text{NO}_3)_2 \cdot 6\text{H}_2\text{O}$  and 75 g  $\text{Al}(\text{NO}_3)_3 \cdot 9\text{H}_2\text{O}$  was put in place of the reflux condenser and the solution was added to the solution in the flask over a 4 h period while maintaining the temperature at <5°C. The resultant slurry was stirred for 1 h at <5°C after which the funnel was removed and the reflux condenser was replaced. The flask was now placed in a Glass Col<sup>®</sup> heating mantle and was

heated to  $60 \pm 5^\circ\text{C}$  for 1 h. The slurry was then cooled to room temperature, the solids recovered by filtration and washed with 10 l of deionized water. These solids were then dried at  $100^\circ\text{C}$  for 16 h. Analysis of this solid by X-ray showed it to be hydrotalcite. After crushing, the solid was calcined at  $450^\circ\text{C}$  for 12 h in a muffle furnace with air flow. This product was characterized as a magnesium–aluminum solid solution by X-ray diffraction and was found to have a surface area of  $285\text{ m}^2/\text{g}$  by the BET technique.

#### 2.1.2. Preparation of $\text{NiO}/\text{Al}_2\text{O}_3$ solid solution

A 2 l, three-necked round bottomed flask was equipped with a reflux condenser, a thermometer, and a mechanical stirrer. To this flask was added a solution containing 412 g of water, 38 g of  $\text{Na}_2\text{CO}_3 \cdot \text{H}_2\text{O}$  and 48.1 g of NaOH and the flask was cooled to  $<5^\circ\text{C}$ . An addition funnel containing 228.4 g water, 100.12 g of  $\text{Ni}(\text{NO}_3)_2 \cdot 6\text{H}_2\text{O}$  and 64.12 g  $\text{Al}(\text{NO}_2)_3 \cdot 9\text{H}_2\text{O}$  was put in place of the reflux condenser and the solution was added to the solution in the flask over a 4 h period while maintaining the temperature at  $<5^\circ\text{C}$ . The resultant slurry was stirred for 1 h at  $<5^\circ\text{C}$  after which the funnel was removed and the reflux condenser replaced. The flask was now placed in a Glass Col<sup>®</sup> heating mantle and was heated to  $60 \pm 5^\circ\text{C}$  for 1 h. The slurry was then cooled to room temperature, the solids recovered by filtration and washed with 10 l of deionized water. These solids were then dried at  $100^\circ\text{C}$  for 16 h. After crushing, the solid was calcined at  $450^\circ\text{C}$  for 12 h in a muffle furnace with air flow. X-ray diffraction analysis showed this product to be a solid solution of nickel and aluminum oxides.

#### 2.1.3. Preparation of $\text{NiO}/\text{MgO}/\text{Al}_2\text{O}_3$ solid solution

A 2 l, three-necked round bottomed flask was equipped with a reflux condenser, a thermometer, and a mechanical stirrer. To this flask was added a solution containing 585 g of water, 60 g of  $\text{Na}_2\text{CO}_3 \cdot \text{H}_2\text{O}$  and 71 g of NaOH and the flask was cooled to  $<5^\circ\text{C}$ . An addition funnel containing 378 g water, 32.5 g of  $\text{Mg}(\text{NO}_3)_2 \cdot 6\text{H}_2\text{O}$ , 110 g of  $\text{Ni}(\text{NO}_3)_2 \cdot 6\text{H}_2\text{O}$ , and 93 g  $\text{Al}(\text{NO}_2)_3 \cdot 9\text{H}_2\text{O}$  was put in place of the reflux condenser and the solution added to the solution in the flask over a 4 h period while maintaining the temperature at  $<5^\circ\text{C}$ . The resultant slurry was stirred for

1 h at  $<5^\circ\text{C}$  after which the funnel was removed and the reflux condenser replaced. The flask was now placed in a Glass Col<sup>®</sup> heating mantle and was heated to  $60^\circ\text{C} \pm 5^\circ$  for 1 h. The slurry was then cooled to room temperature, the solids recovered by filtration and washed with 10 l of deionized water. These solids were then dried at  $100^\circ\text{C}$  for 16 h. After crushing the solid was calcined at  $450^\circ\text{C}$  for 12 h in a muffle furnace with air flow. X-ray diffraction analysis showed this product to be a solid solution of nickel, magnesium and aluminum oxides. This sample had a BET surface area of  $199\text{ m}^2/\text{g}$ .

### 2.2. Catalyst preparation

The catalysts used in this work were prepared by evaporative impregnation of the MOSS with a methanolic solution of sulfonated cobalt phthalocyanine (S-CoPc) (1 ml of methanol was used for each ml of support, target Cobalt level of 500 ppm). The MOSS support was placed in a rotary evaporator with methanol and S-CoPc and dried for 1 h at ambient temperature. They were then dried for another hour with low pressure steam passing through the steam jacket of the rotary evaporator.

### 2.3. Characterization

The LDHs and the MOSS were characterized using standard XRD techniques. Other characterization included surface area measurements as well as bulk chemical analysis and thermogravimetric analysis (TGA). Sample homogeneity, especially in the ternary system (Mg–Ni–Al), was determined by using scanning electron microscopy (SEM).

### 2.4. AcAc test

The acid and base characteristics of the catalysts used in this study were evaluated using the probe reaction reported by Dessau [11]. In this system, acetonylacetone (AcAc) is heated in the presence of the test catalyst. One or two possible products can form depending on the basic or acidic nature of the catalyst. These products are presented in Fig. 3.

The reaction was carried out in a pulse-flow micro-reactor in which 2 ml of AcAc was passed over 1 g of catalyst at  $350^\circ\text{C}$  in flowing nitrogen. The reaction

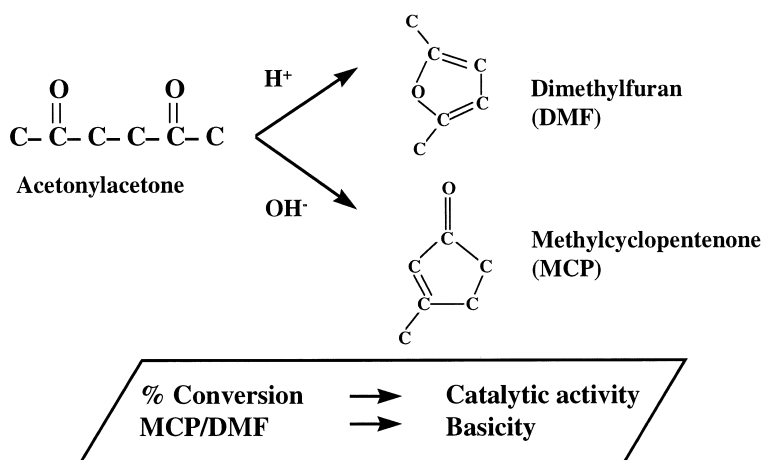


Fig. 3. Chemistry of acetonylacetone microreactor test.

products were collected downstream of the reactor in a cold trap and analyzed by gas chromatography (GC). The selectivity of the sum of both products is  $\sim 90\%$ . The ratio of the two selectivities is used as an indication of base vs. acid catalytic activity

$$\frac{\text{selectivity to MCP}}{\text{selectivity to DMF}} = \text{base vs. acid activity}$$

If this ratio is  $\gg 1$ , the catalyst is basic; if the ratio is  $\ll 1$ , the catalyst is acidic. If the ratio is of the order of magnitude of  $\sim 1$ , the catalyst has both acid and base

properties. The acidity and basicity of several solid materials as measured by this technique are presented in Fig. 4. Silica–alumina, beta zeolite, and ZSM-5 are seen to be primarily acids; CsX has primarily basic sites; and K/graphite, NaK/alumina and MOSS have exclusively strong base sites.

## 2.5. Bench test

A bench test was developed for easy measurement of catalyst activity. For this test, a synthetic feed was

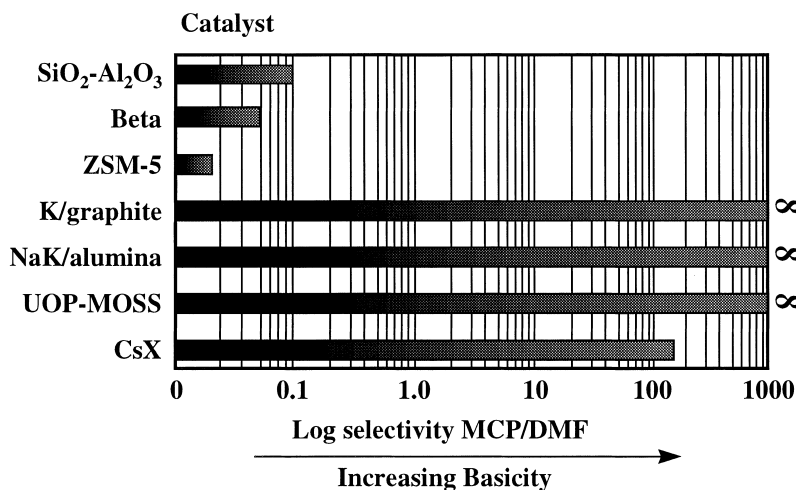


Fig. 4. Selectivity for various materials in the AcAc test. Note that acidic materials show little MCP formation, and that the basic materials do not form any DMF.

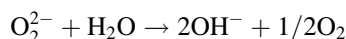
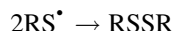
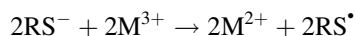
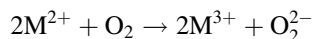
prepared by adding 1-octane thiol to iso-octane to achieve a mercaptan sulfur level of 1000 ppm. The catalyst (0.8 g) and dry methanol (1 ml) were added to 50 g of the feed mixture in a Morton flask. The slurry was stirred vigorously. After the designated reaction time, generally 1 h, the catalyst was separated from the liquid phases by filtration. The methanol phase was removed by using a separatory funnel, and the resulting hydrocarbon solution was submitted for mercaptan analysis.

### 2.6. Pilot plant

The plant used a fixed-bed reactor that would accommodate 25–100 ml of catalyst (Fig. 5). A suitable temperature control system was used to allow operation at near-ambient temperature. The feed system consisted of three parts: an air feed system, a kerosene or gasoline feed system, and a water feed system. All three feed components: kerosene, air, and water, were mixed thoroughly prior to entering the reactor. The product was separated into three phases, and the hydrocarbon phase was analyzed for mercaptan level and acid number.

## 3. Results and discussion

The mechanism of mercaptan oxidation can be summarized as [12]



The first step is of primary relevance to this work. The formation of a mercaptide ion from the mercaptan is necessary as the first step in the reaction. Traditionally the formation of the mercaptide has been promoted by adding an aqueous base such as sodium hydroxide or ammonia. In this work, we use a solid base to provide this function. The subsequent oxidation of the mercaptide is catalyzed by the transition metal present in the catalyst system, frequently a metal phthalocyanine. This oxidation mechanism is complex and is beyond the scope of this work.

Bench tests were conducted using samples prepared by impregnation or intercalation of S-CoPc [13] into LDH or calcined LDH samples. The results are shown in Fig. 6. The catalyst prepared by impregnating S-CoPc onto a calcined LDH was effective at converting mercaptan to disulfides, but the intercalated samples gave almost no conversion.

The flaw in preparing the samples by intercalation is that both an active oxidation component (CoPc) and a base function (MOSS) must exist at the same time. The CoPc intercalated into an LDH has no strong base

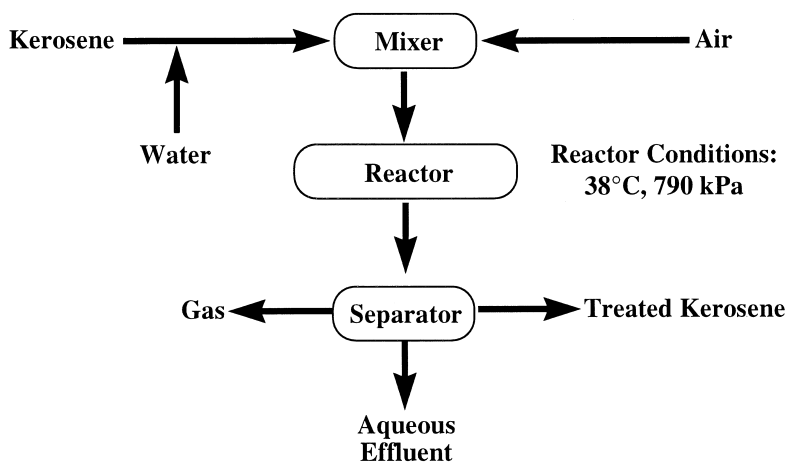


Fig. 5. Pilot plant schematic.

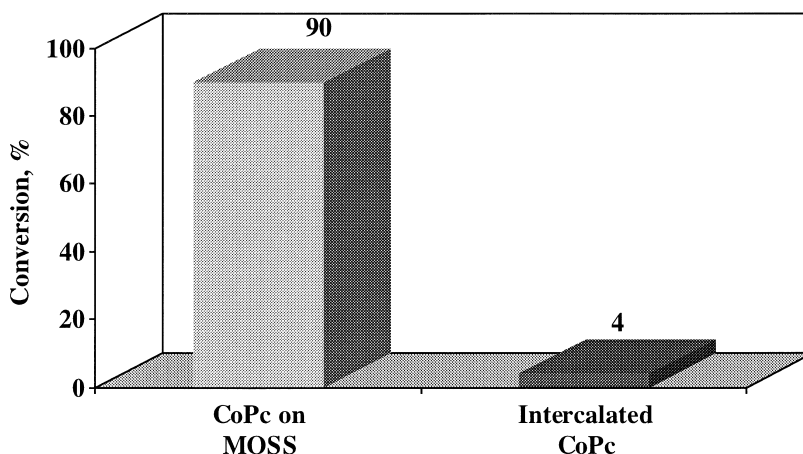


Fig. 6. Conversion of *t*-dodecyl mercaptan (1000 ppm S) in isooctane.

function until it is converted into the highly basic MOSS form by calcination. Unfortunately, this calcination step destroys the oxidation function by decomposing the CoPc complex.

### 3.1. Gasoline testing

Tests were conducted to determine if MOSS could be used as the base function for treating gasoline (Fig. 7). In these studies, fluid catalytic cracking (FCC) gasoline with a mercaptan level of 149 ppm sulfur was used. The catalyst was treated at 3 and 5 LHSV. At these conditions, when sufficient air was used, greater than 99% of the mercaptans were converted to disulfides. Since gasoline feeds are relatively clean, no catalyst deactivation was observed.

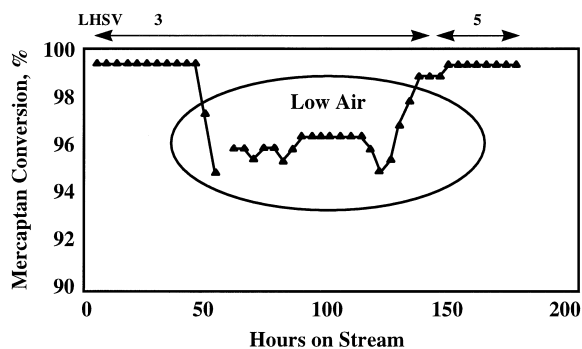


Fig. 7. Mercaptan oxidation of gasoline using CoPc/(3:1)Mg–Al MOSS (318 ppm Co).  $O_2/RSH=0.5$ ; feed RSH=149 ppm S.

### 3.2. Kerosene testing

Gasoline treatment with MOSS-based catalysts was successful, and so the next step was to treat kerosene. The first test was conducted with a commercial kerosene. In this test, Mg–Al MOSS impregnated with S–CoPc was used. Kerosene was used without any pretreatment. The catalyst deactivated significantly over 120 h, as demonstrated in Fig. 8. For comparison, Fig. 9 shows the results of testing the stability of Caustic-Free Merox treating. In this test, the catalyst was stable for more than 1500 h.

These results led to the consideration of what pathways could cause such rapid deactivation when kerosene is used as no deactivation occurs when gasoline is used. Three potential deactivation mechanisms were

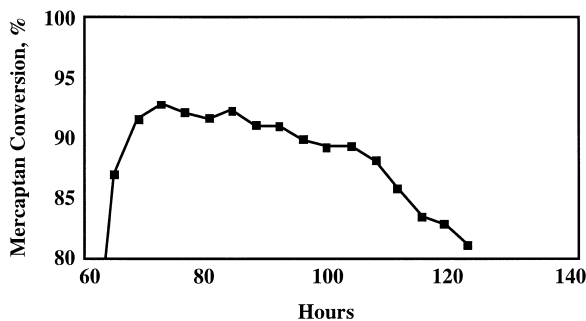


Fig. 8. Mercaptan oxidation of kerosene using CoPc/(3:1)Mg–Al MOSS (750 ppm Co).  $O_2/RSH=0.5$ ; feed RSH=162 ppm S; 1.3 LHSV.

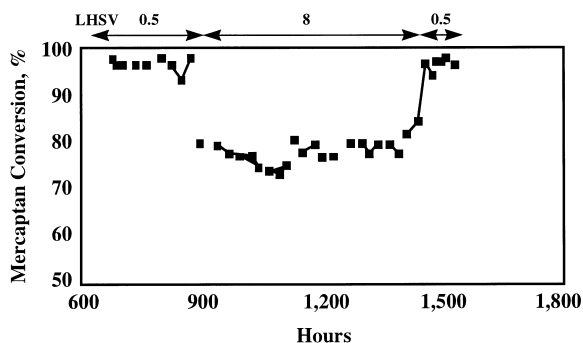


Fig. 9. Mercaptan oxidation of kerosene using UOP Caustic-Free Merox™ process.  $O_2/RSH=0.75$ ; feed  $RSH=141$  ppm S.

identified: rehydration of the MOSS back to the LDH form, poisoning of the base sites by the acids (primarily naphthenic acids) present in kerosene, and fouling caused by heavy hydrocarbon components in the kerosene.

### 3.2.1. Rehydration

MOSS are known to rehydrate back to LDHs when exposed to water (Fig. 10). This phenomenon, which is reversible, is also observed for MgO. Surface area and basicity measurements show that the MOSS has

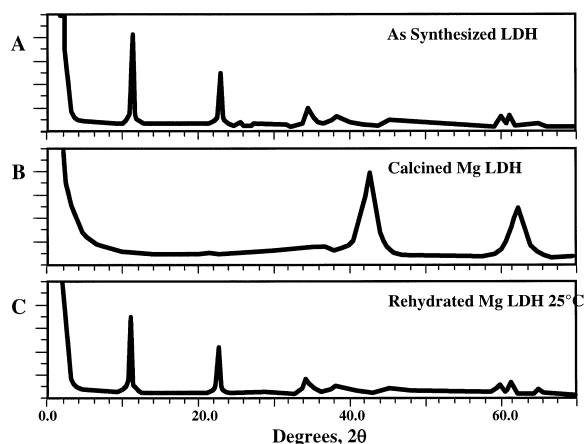


Fig. 10. The XRD patterns show the impact of calcination and rehydration on a Mg/Al layered double hydroxide. On calcination, the sample is converted to the Mg–Al MOSS. This conversion is reversible on rehydration as shown by the rehydrated pattern, C.

the higher surface area and higher basicity (Fig. 11). Therefore, because the MOSS is the active species, rehydration to the LDH should result in a loss of activity. When the MOSS rehydrates during use, the net result is a loss of activity. The XRD spectra of spent catalysts show that during use, the samples rehydrate to the LDH.

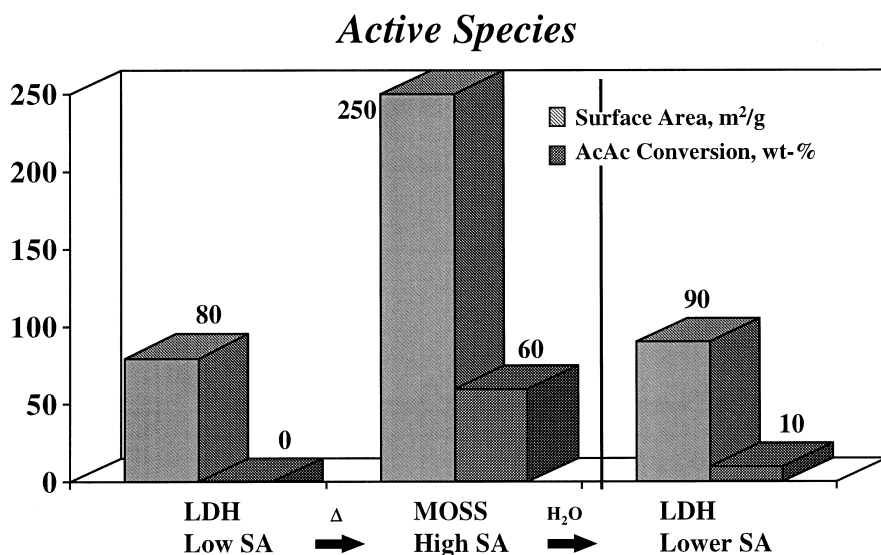


Fig. 11. The conversion of a Mg–Al LDH to a Mg–Al MOSS is accompanied by an increase in surface area (SA) and conversion in the AcAc test. If the sample is rehydrated back to the starting Mg–Al LDH, a concomitant reduction in surface area and AcAc conversion is observed.



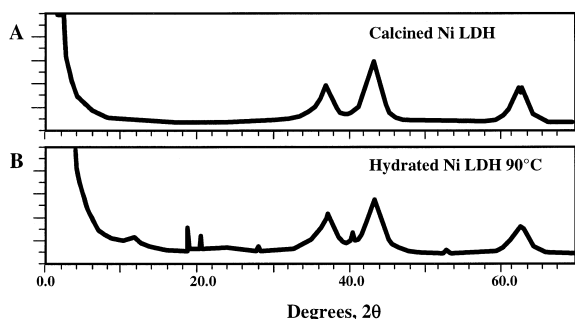


Fig. 12. This figure shows the impact of rehydration on a Mg–Ni–Al MOSS. Note that the XRD pattern is substantially unchanged, suggesting only minor rehydration back to the starting LDH. The additional XRD peaks are due to the formation of small amounts of Gibbsite by recrystallization of non-framework Al during the rehydration process.

This problem can be solved by going to a composition with stronger metal-oxide bonds. The result is a material that is not as susceptible to rehydration. Samples containing various amounts of Mg, Ni, and Al were prepared. Data show that the ternary MOSS phases, Mg–Ni–Al, do not rehydrate even when refluxed in the presence of water for 16 h (Fig. 12). This MOSS material can be used as a support for CoPc. In the case of gasoline sweetening, this change to the Mg–Ni–Al MOSS ternary material is sufficient to stop deactivation if water is used.

### 3.2.2. Naphthenic acid poisoning

As MOSS materials are solid bases, it may be reasonably assumed that they will adsorb any acids passed over them. This neutralization reaction decreases the number of base sites available for catalysis. Thus, any acids in the feed stream should be expected to deactivate the catalyst.

Kerosene generally contains naphthenic acids which are present in relatively low concentration: acid numbers of 0.01–0.1 mg KOH/g of hydrocarbon. The naphthenic acid is therefore likely to act as a slowly building poison to any solid base it passes over.

Naphthenic acid poisoning was investigated by adsorbing naphthenic acid onto a MOSS sample and then measuring the activity in a stirred contact test. For the test, 0.8 g of catalyst was stirred for 1 h with 1 ml of dry methanol and 50 g of 1000 ppm 1-octane thiol in iso-octane. The results are presented in Fig. 13. These results indicate that S-CoPc/Ni–Al MOSS is deactivated by adsorbing naphthenic acid. The same catalyst was washed with 100 ml of water at 90°C. The regenerated catalyst had an activity near that of the fresh catalyst.

In addition to these bench tests, a test was conducted in the pilot plant using kerosene that contained naphthenic acids. In this test, the acid number was measured in the product stream. This test determined the amount of acid that was irreversibly adsorbed onto the catalyst. The results in Fig. 14 show that acid was

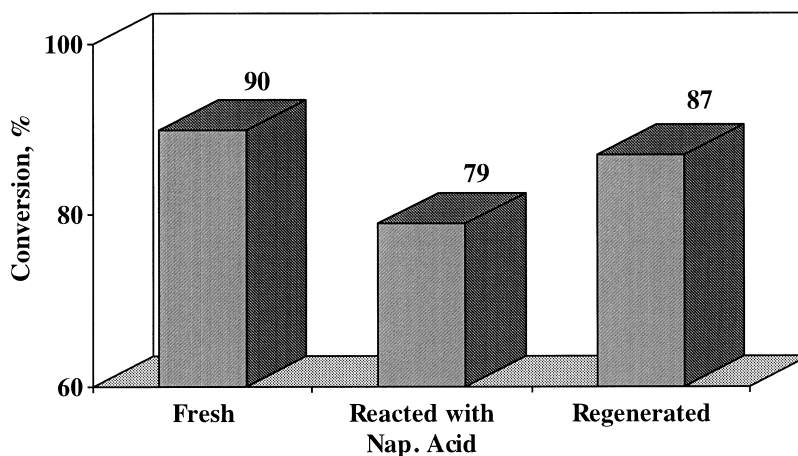


Fig. 13. Conversion of *t*-dodecyl mercaptan (1000 ppm S) in isooctane.

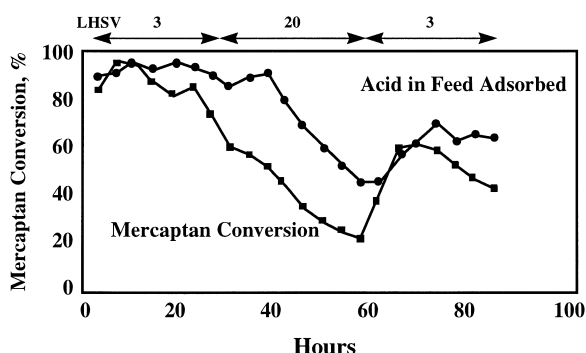


Fig. 14. Mercaptan oxidation of kerosene using CoPc/(2:1){25%Ni, 75%Mg}-Al MOSS (507 ppm Co).  $O_2/RSH=0.5$ ; feed RSH=381 ppm S.

continuously adsorbed by the catalyst. As a result, the base sites were poisoned and catalyst deactivation occurred.

### 3.2.3. Fouling

A test was conducted using a CoPc/Ni MOSS catalyst that could not rehydrate and a kerosene feed that had been washed to remove all acids. The test ran for 110 h. A deactivation of greater than 50% was observed. This result indicated that a third deactivation mechanism was occurring. On the basis of the previous sweetening experience, the catalyst can deactivate by adsorption of heavy hydrocarbon species typically present in kerosene. Although no experiments were conducted to prove that this mechanism occurs with this catalyst system, a quaternary ammo-

niun salt was injected with the aqueous stream to solubilize any heavy species that would accumulate on the surface.

Once all of the deactivation mechanisms were understood, all of the solutions were applied at one time to determine catalyst stability. In this run, the kerosene was washed with a sodium hydroxide solution to remove all acidic poisons. A Ni-Mg-Al MOSS support was used to prevent any rehydration caused by the water present. Finally, a quaternary ammonium salt was continuously injected to eliminate the buildup of heavy hydrocarbon species on the catalyst surface. As a result of all these procedures, the catalyst stability improved significantly. The results are presented in Fig. 15.

## 4. Conclusion

Solid bases formed from calcination of LDHs were successfully used to replace caustic in the oxidation of mercaptans to disulfides [14–16]. The FCC gasoline was easily treated with CoPc supported on a Mg-Al MOSS. Kerosene could also be treated with a similar catalyst system. However, several components present in kerosene that are not present in gasoline complicated the process. The use of water necessitated the development of a basic solid oxide that would not rehydrate to the parent LDH. This problem was solved by adding nickel to the formulation. Also, the acid species present in kerosene must be removed prior to treatment to prevent them from adsorbing strongly onto the base sites. Finally, the addition of a surfactant was necessary to prevent the buildup of heavy hydrocarbon species on the catalyst surface.

In the competitive refining environment of the 1990s, each refiner must be aggressive in search for ways to decrease operating costs. Minimizing waste and maximizing the use of resources is fundamental to this goal. Eliminating the use of caustic and the accompanying need to pay for its disposal is a specific application of this approach. The use of a solid base catalyst for mercaptan oxidation results in an effluent-free system. Under the right circumstances of economics and environmental demands, the solid base system can be applied to the practical problem of sweetening FCC gasoline in the refinery.

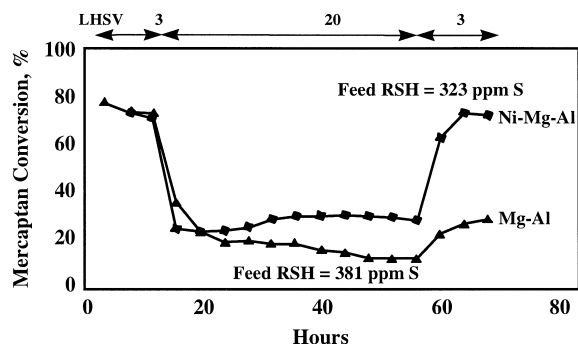


Fig. 15. Mercaptan oxidation of kerosene using CoPc/(3:1)Mg-Al MOSS (524 ppm Co) and CoPc/(2:1)Ni-Al MOSS (592 ppm Co).  $O_2/RSH=0.5$ ; feed RSH=381 ppm S.

## Acknowledgements

The authors would like to acknowledge Bruce Berntzen, Phil Coglio, and John Leon for help with the pilot plant studies; Shawn Clisham for the AcAc conversion studies; Sung Jeon and Geralyn Schroeder for laboratory experiments; Judy Triphahn for XRD; Dave Holbrook for many helpful discussions; and finally Barry Ferm for his contributions to the entire project.

## References

- [1] D.L. Holbrook, in: R.A. Meyers (Ed.), *Handbook of Petroleum Refining Processes*, 2nd ed., Chap. 11.3, McGraw Hill, New York, 1997.
- [2] H. Pines, *Base-catalyzed Reactions of Hydrocarbons and Related Compounds*, 1977.
- [3] W.T. Reichle, *J. Catal.* 94 (1985) 547–557.
- [4] S. Miyata, *Clays and Clay Minerals* 23 (1975) 369–375.
- [5] W. Feitknecht, W. Lotmar, *Z. Kristallogr.* 91 (1935) 136–141.
- [6] W. Feitknecht, *Z. Agnew. Chem.* 49 (1936) 24–25.
- [7] W. Feitknecht, *Helv. Chim. Acta* 21 (1938) 766–784.
- [8] W.T. Reichle, *Chemtech*, (1986) 58–63.
- [9] C. Misra, A. Perrotta, *Clays and Clay Minerals* 24 (1992) 145–150.
- [10] F. Cavani, F. Trifiro, A. Vaccari, *Catal. Today*, (1991) 11–173.
- [11] R.M. Dessau, *Zeolites* 10 (1990) 205–206.
- [12] T. Wallace, A. Schriesheim, H. Hurwitz, M. Glaser, *Ind. Eng. Chem. Proc. Des. Dev.* 3 (1964) 237–241.
- [13] M. Perez-Bennal, R. Rueno-Casero, T. Pinnavaia, *Catal. Lett.* 11 (1991) 55–62.
- [14] R. Gillespie, J. Bricker, B. Arena, J. Holmgren, US Patent 5,593,932.
- [15] B. Ferm, B. Arena, J. Holmgren, US Patent 5,401,390.
- [16] R. Gillespie, J. Bricker, B. Arena, J. Holmgren, US Patent 5,413,704.